

# 1 **Photolysis of frozen iodate salts as a source of active** 2 **iodine in the polar environment**

3

4 **Óscar Galvez<sup>1</sup>, M. Teresa Baeza-Romero<sup>2</sup>, Mikel Sanz<sup>2</sup> and Alfonso Saiz-Lopez<sup>3</sup>**

5 [1]{Departamento de Física Molecular, Instituto de Estructura de la Materia, IEM-CSIC,  
6 28006 Madrid, Spain}

7 [2]{Escuela de Ingeniería Industrial, Universidad de Castilla-La Mancha, 45071, Toledo,  
8 Spain}

9 [3]{Department of Atmospheric Chemistry and Climate, Institute of Physical Chemistry  
10 Rocasolano, CSIC, 28006 Madrid, Spain}

11

12 Correspondence to: O. Gálvez ([oscar.galvez@csic.es](mailto:oscar.galvez@csic.es))

13

## 14 **Abstract**

15 Reactive halogens play a key role in the oxidation capacity of the polar troposphere.  
16 However, sources and mechanisms, particularly those involving active iodine, are still poorly  
17 understood. In this paper, the photolysis of an atmospherically relevant frozen iodate salt has  
18 been experimentally studied using infrared (IR) spectroscopy. The samples were generated at  
19 low temperatures in the presence of different amounts of water. The IR spectra have  
20 confirmed that under near-UV/Vis radiation iodate is efficiently photolyzed. The integrated  
21 IR absorption coefficient of the iodate anion on the band at  $750\text{ cm}^{-1}$  has been measured to be  
22  $A=9.5\times 10^{-17}\text{ cm molec}^{-1}$ . Monitoring the decay of ammonium IR band ( $1430\text{ cm}^{-1}$ ) in the  
23 presence of a solar simulator, which was observed to correlate with iodate anion IR band,  
24 photolysis rate of ammonium iodate salt was measured. A lower limit of the integrated  
25 absorption cross section of iodate, in an ammonium frozen salt, has been estimated for the  
26 first time at wavelengths relevant for tropospheric studies ( $(1.1\pm 0.6)\times 10^{-20}\text{ cm}^2\text{ nm}$  from 300  
27 to 900 nm). According to this, we suggest that the photolysis of iodate in frozen salt can  
28 potentially provide a pathway for the release of active iodine to the polar atmosphere.

29

## 1 **1 Introduction**

2 Atmospheric iodine compounds are present in the marine and polar boundary layers (Saiz-  
3 Lopez et al., 2012), where it plays a relevant role in catalytic ozone destruction (Saiz-Lopez et  
4 al., 2007b) (Read et al., 2008) and could also be involved in new particle formation in the  
5 polar environment (Allan et al., 2015;Roscoe et al., 2015). Moreover, in the polar atmosphere,  
6 iodine has also been suggested as one of the possible sinks of gaseous elemental mercury  
7 (Calvert and Lindberg, 2004;Saiz-Lopez et al., 2008).

8 Despite the concentration of atmospheric iodine being highly variable at different regions,  
9 ground- (Frieß et al., 2001) (Saiz-Lopez et al., 2007b) (Atkinson et al., 2012) and satellite-  
10 based instrumentation (Saiz-Lopez et al., 2007a;Schönhardt et al., 2008) measurements have  
11 confirmed remarkably high concentrations (up to 20 pptv) of IO in coastal Antarctica.  
12 Nevertheless, the sources and mechanisms of iodine emissions from ice remain poorly  
13 understood (Saiz-Lopez et al., 2015;Kim et al., 2016).

14 Apart from observations of gaseous iodine species, different studies have conducted analysis  
15 of the iodine fraction in rainwater (Laniewski et al., 1999) and aerosol (Baker et al., 2000). In  
16 all of them, iodine concentrations are considerably enriched over seawater, and an appreciable  
17 fraction of soluble iodine species like  $I^-$  and  $IO_3^-$  is observed, although the mechanism  
18 determining the  $I^-/IO_3^-$  ratio is still unclear. Thus, for example since  $IO_3^-$  has been considered  
19 an inert inorganic iodine species, and therefore a sink molecule in the atmospheric iodine  
20 cycle, model calculations (Pechtl et al., 2006) suggest that  $IO_3^-$  should accumulate in marine  
21 aerosol. However, several field campaigns (Baker, 2004;Gilfedder et al., 2008) have revealed  
22 that the iodide/iodate ratio is rather variable in aerosol, showing significant  $I^-$  concentration.

23 A recent study has suggested that  $IO_3^-$  anions show a substantial reactivity in frozen solutions  
24 under near-UV/Visible light irradiation (Spolaor et al., 2013). During the irradiation of  $IO_3^-$   
25 solutions reactive gaseous iodine species were produced and converted to iodine oxide  
26 particles (IOP) for detection. Inspired by these results, we have further studied the photo-  
27 stability of iodate frozen salts to assess its potential role in iodine emissions to the polar  
28 atmosphere. In this work, we have determined for the first time the integrated absorption cross  
29 section of frozen ammonium iodate solutions at wavelengths relevant for the troposphere.  
30 Using this value (which should be taken as a lower limit that need to be confirmed in future  
31 works), and the recorded UV-Vis spectra for the liquid solution, we have also simulated the  
32 differential absorption cross section from 300 to 900 nm. This information has been

1 incorporated into an atmospheric model of the Antarctic boundary layer to assess the potential  
2 of iodate photolysis to release reactive iodine in coastal Antarctica during springtime.

3

## 4 **2 Experimental methods**

5 For the study of the photolysis of iodate salts, we have chosen aqueous solutions of  $\text{NH}_4\text{IO}_3$ .

6 The choice of this species was based on several reasons:

7 (i) It was not possible to monitor iodate signal in the presence of high concentration of water  
8 since the infrared iodate band overlaps with water absorptions. The fact that the chosen salt  
9 has a cation like  $\text{NH}_4^+$  that presents a band with no interference (and that it is consumed in a  
10 1:1 ratio with iodate) allowed us to measure the photolysis of iodate indirectly as described  
11 below.

12 (ii) The integrated IR absorption coefficient of iodate band was unknown, and in  
13 consequence, it was not possible to quantify the amount of iodate in the samples. One of the  
14 possibilities to solve this problem is to use an iodate salt for which the integrated absorption  
15 coefficient of the IR band of the counter-ion was known, like ammonium iodate. More details  
16 of these calculations are given in the next section.

17 (iii) Moreover, ammonium iodate is expected to be one of the abundant iodate salts in the  
18 atmosphere, since ammonium concentrations are high in some environments, and it could be  
19 deposited into the ice as large fluxes of iodinated compounds have been observed during  
20 glacial period (Spolaor et al., 2013), and the presence of ammonium ions in ice samples is  
21 also expected. Moreover, ammonium and iodinated compounds have been detected at the  
22 same time in melting Arctic sea ice, implying that this salt could be atmospherically relevant  
23 (Assmy et al., 2013).

24 However, other salts like  $\text{NaIO}_3$  or  $\text{KIO}_3$  would be representative of polar environments also,  
25 and further experiments using these compounds should be addressed in the future.

26 Solid samples containing iodate anions were produced through the sudden freezing of droplets  
27 of aqueous solutions of  $\text{NH}_4\text{IO}_3$  on a cold Si substrate located inside a vacuum chamber. A  
28 detailed description of the experimental setup can be found elsewhere (Maté et al.,  
29 2009;Gálvez et al., 2010), and only a brief description of the most relevant aspects for the  
30 present experiments is given here. The solid substrate is mounted in a Cu block in contact  
31 with a liquid nitrogen Dewar. The substrate temperature can be controlled with 1 K accuracy

1 between 90 K and 300 K. The vacuum chamber, which is coupled to a Vertex70 Bruker FTIR  
2 spectrometer through a purged pathway, is evacuated with a turbomolecular pump to a  
3 background pressure of  $\sim 10^{-8}$  mbar. Transmission spectra of the samples were recorded, with  
4  $2\text{ cm}^{-1}$  resolution, using an MCT (Mercury Cadmium Telluride) detector refrigerated with  
5 liquid nitrogen. Liquid solution droplets from a room temperature pulsed valve (General  
6 Valve, series 9), usually employed for the generation of free jets and molecular beams (Abad  
7 et al., 1995), were made to impinge on the cold Si substrate placed at  $\sim 15\text{-}20$  mm. When a  
8 desired amount of sample is on the substrate, this can be rotated to record the IR spectra, or to  
9 be processed by simulated Solar light. A scheme of the experimental setup is shown in Fig. 1.  
10 Solar irradiance was simulated by a 1000 W LOT® Xenon Arc lamp that radiate between  
11 around 250 nm to  $2.5\text{ }\mu\text{m}$ , although an important fraction of the output is given below 900 nm  
12 according to the supplier of this lamp, where a fairly constant spectral irradiance is obtained  
13 between 300 to 900 nm. Power light received on the substrate is measured by a portable meter  
14 Thermal Detector, model 407A by Spectra-Physics, which operates in a wavelength range  
15 from 250 nm to  $11\text{ }\mu\text{m}$  without significant sensitivity variations (less than 3 %).

16 UV-Vis spectra of studied salts were obtained in water solution at different concentrations  
17 using an UV-Visible Uvikon spectrophotometer 930 from Kontron Instruments equipped with  
18 quartz cuvettes of 10 mm size. The spectra resolution was fixed at 0.5 nm, from 190 to 500  
19 nm.

20 In all experiments, pulsed valve was filled by a solution 0.1 M of ammonium iodate (Across  
21 Organics, for analysis). A slight He overpressure behind the liquid solution filling the valve  
22 improved the performance. This generation procedure does not lead to a uniform film, and the  
23 thickness of the ice samples, which typically range from 0.1 to  $1\text{ }\mu\text{m}$  approximately (Mate et  
24 al., 2012), can vary among different experiments. Solid samples generated by this technique  
25 contain compact ices structures in a hyperquenched glassy water morphology (Mayer, 1985)  
26 in which the water molecules retain their amorphous liquid structure, and where ions are  
27 solvated by water molecules instead of being segregated in the ice (Mate et al., 2012). When  
28 the temperature of substrate is below water sublimation (around 170 K), the concentration of  
29 ammonium iodate salt in the ices samples is very low (comparable to the liquid solution), and  
30 infrared spectra of these ice mixtures are dominated by water absorptions. In these cases,  
31 water bands hide the IR features of the salt, and prevent monitoring its evolution during  
32 irradiation. For this reason, most of the samples are slowly warmed above water sublimation

1 to achieve a lower water concentration to avoid that problem, or just to study dry samples  
2 (although an amount of water is always present). Nevertheless, some samples were also  
3 reserved in their original diluted salt proportion to explore this possible variable. We refer to  
4 the samples that have suffered this process as *hyperquenched (HQ) samples*. In other  
5 experiments, samples are dry, and then a controlled water vapour flux is added to be adsorbed  
6 on the salt, which was kept at low temperatures (100 or 140 K) to condense water. With this  
7 procedure, solid samples present a different morphology since water molecules are deposited  
8 uniformly on the salt surface resulting in a more porous structure. When the condensation of  
9 water occurs at 100 K, a homogeneous film of low-density amorphous water ice is deposited  
10 on top of the salt. If the temperature of deposition is 140 K, the ice film has crystal cubic ice  
11 structure (Mate et al., 2012). In both cases, we refer to these samples as *Vapor deposited*  
12 *(Vap) samples*.

13 Initially, and it has been mentioned above, deposition at low temperature ( $< 120$  K) leads to  
14 amorphous ices samples, which show high specific surface areas (SSA) (Mate et al., 2012),  
15 around 100 times higher, or even more, than typical atmospheric ice samples. However, when  
16 temperature is increased amorphous samples are irreversibly transformed to cubic crystal ice,  
17 leading to a reduction of the SSA by a factor of 100 or even higher (Ocampo and Klinger,  
18 1982), which are common values of freshly atmospheric ice samples.

19 Due to the requirements of the experimental setup, the ratio of  $\text{NH}_4\text{IO}_3:\text{H}_2\text{O}$  in the samples is  
20 considerable much higher than for environmental ices, however, some more diluted samples  
21 has been studied to see the effect of this variable in the photolysis process, although always  
22 our samples were much more concentrated than in natural polar conditions.

23 To summarize the procedure to generate the samples, they were firstly generated by HQ  
24 deposition at 100, 140, 160, 200, 260 or 298 K. After deposition at those temperatures, three  
25 different processes could be carried out: (i) the samples at the deposition temperature were  
26 just irradiated, (ii) samples were firstly annealing to eliminate part of the water, then cold  
27 down to a certain temperature and then irradiated, (iii) or samples were annealing until to be  
28 completely dry, then cold down to a selected temperature at which a certain amount of water  
29 from vapor phase was deposited, and finally irradiated.

## 1 **2.1 Determination of the concentration of species in the samples**

2 Column densities of water,  $\text{NH}_4^+$  and  $\text{IO}_3^-$  ions in the ice mixtures were calculated via the  
3 Lambert–Beer equation, using the integrated values of the infrared absorption bands, and the  
4 corresponding integrated absorption coefficients,  $A$ . The bands chosen for this purpose were  
5 the  $\nu_2$  and  $\nu_2+\nu_R$  bands of water around 1650 and 2220  $\text{cm}^{-1}$ , respectively, the  $\nu_4$  band of  
6  $\text{NH}_4^+$  around 1430  $\text{cm}^{-1}$ , and the  $\nu_3$  band of  $\text{IO}_3^-$  at approx. 740  $\text{cm}^{-1}$ . For water band intensity,  
7 we have used the values reported by Mastrapa *et al.* (Mastrapa *et al.*, 2009) for an amorphous  
8 or crystalline (cubic) phase at 100 K. For *HQ* samples the values of amorphous ice are used:  
9  $A(\text{H}_2\text{O})_{\text{amorphous}} = 1.6 \times 10^{-17}$  and  $9.8 \times 10^{-18}$   $\text{cm molec}^{-1}$ , while for *Vap* samples the integrated  
10 absorption coefficients of cubic ice are more representative:  $A(\text{H}_2\text{O})_{\text{cubic}} = 1.8 \times 10^{-17}$  and  $1.1$   
11  $\times 10^{-17}$   $\text{cm molec}^{-1}$ , for 1650 and 2220  $\text{cm}^{-1}$  bands, respectively. In the case of  $\text{NH}_4^+$ , different  
12 values of the absorption coefficient have been reported in the literature, ranging from 2.5 to  
13  $4.4 \times 10^{-17}$   $\text{cm molec}^{-1}$  (Maté *et al.*, 2009) (Schutte and Khanna, 2003). Due to these  
14 discrepancies, we have selected a suitable value of  $4.0 \times 10^{-17}$   $\text{cm molec}^{-1}$ , close to that given  
15 by Schutte & Khanna (Schutte and Khanna, 2003) for solid samples, which are more  
16 representative of our case. For iodate, we are not aware of previous data of  $A$  values in the IR  
17 region. In this case, we have estimated this value for pure ammonium iodate samples, based  
18 on that previously given for  $\text{NH}_4^+$ , obtaining a mean integrated absorption coefficients  $A(\text{IO}_3^-)$   
19  $= 9.5 \times 10^{-17}$   $\text{cm molec}^{-1}$  for the band centred at 750  $\text{cm}^{-1}$ .

## 20 **2.2 Calculation of spectral irradiance received by the samples**

21 We assumed that the observed photolysis of ammonium iodate samples should be mainly due  
22 to the highest frequency photons emitted by the Solar lamp. The reason is that  $\text{IO}_3^-$  in aqueous  
23 media absorbs light only in the UV range (Awtrey and Connick, 1951), at wavelengths below  
24 270 nm, which is also in agreement with our near UV-Vis spectra of iodate salts (see Fig. 2).  
25 In consequence, the UV-Vis spectrum of the glass window, through which light penetrates  
26 before reaching the sample (see Fig. 1), was recorded to demarcate the transparent interval of  
27 frequencies, especially the UV cutoff, see Fig. 2. Taking into account this spectrum, and in  
28 combination with that provided by the lamp manufacturer for the lamp spectra and spectral  
29 irradiance at 0.5 m, we estimated that only 42% of the total lamp power is emitted in the  
30 wavelength interval from 300 to 900 nm. Consequently, since our Thermopile covers the  
31 whole range of frequencies without significant variations, only a 42 % of the measured power

1 is due to the impinged photons of 300 to 900 nm. The average reading in the Thermopile  
2 along the experiments was around  $1.5 \text{ W cm}^{-2}$ , which was regularly monitored during the  
3 experiments. Thus, according to the above estimation, the substrate was irradiated with an  
4 average light power of  $0.66 \text{ W cm}^{-2}$ , in the wavelength range of 300 to 900 nm. In order to  
5 illustrate whether this irradiance power is characteristic of environmental conditions, we  
6 estimated that around  $2.8 \times 10^{15} \text{ photons cm}^{-2} \text{ s}^{-1}$  are impinging the substrate at 500 nm, which  
7 result in around 8 times higher irradiance than the measured mean Solar irradiance on Earth  
8 surface at mid-latitudes, ca.  $3.5 \times 10^{14} \text{ photons cm}^{-2} \text{ s}^{-1}$ . Nevertheless, we take into account  
9 that, due to our experimental procedure, samples are not homogeneously distributed on the  
10 substrate, and consequently the photon flux impacting on the samples was, to a certain degree,  
11 lower. This consideration is further explored in the following section.

12

### 13 **3 Results and Discussions**

#### 14 **3.1 Laboratory experiments**

15 Fig. 3 shows IR spectra of different samples of solid ammonium iodate salt at 200 and 100 K  
16 including those of 3.6 and 2.1  $\text{H}_2\text{O}/\text{NH}_4\text{IO}_3$  ice mixtures deposited at 100 K obtained by the  
17 hyperquenching (*HQ*) technique or via vapor deposited (*Vap*)  $\text{H}_2\text{O}$ , respectively. Table 1  
18 displays the positions of bands of the IR spectra of  $\text{NH}_4\text{IO}_3$  shown in Fig. 3. Sharper and more  
19 defined bands appear in spectra at 100 K, showing also a slight displacement, which are  
20 typical effects when temperature is decreased (Gálvez et al., 2009). When water is present,  
21  $\text{IO}_3^-$  bands undergo a small blue-shift, which can be related to the overlap with the  $\nu_{\text{R}}$  libration  
22 water mode at ca.  $800 \text{ cm}^{-1}$ . Moreover, some differences in the water bands become visible on  
23 the spectra of the mixtures, arising from the solid structure of water ice. In the *HQ* sample  
24 show in the figure, the initial deposited ice mixture at 100 K is slightly warmed to 200 K to  
25 dry the sample and to achieve the water/salt composition desired and then cold down to 100 K  
26 for recording the spectrum. Therefore, in this process, initial amorphous water matrix is  
27 crystallized during annealing, showing an IR spectrum typical of a cubic phase. In the case of  
28 *Vap* samples, initial deposits at 100 K are completely dried at high temperature, and, after  
29 decreasing to 100 K, water is added at this temperature to achieve the water/salt composition  
30 required. Therefore, in this case, water ice shows a low-density amorphous structure, which  
31 corresponds to deposition at 100 K, showing broader bands in the IR spectrum.

1 After generation, samples were irradiated during 3 to 5 hours by a 1000 W Xenon Arc lamp.  
2 This process has been carried out for all samples generated by means of the different  
3 procedures mentioned in the experimental section. In all samples  $\text{NH}_4^+$  and  $\text{IO}_3^-$  IR bands  
4 diminish during irradiation process, which is especially evident when 1430 and  $745\text{ cm}^{-1}$   
5 bands are monitored. The photo-reduction of iodate in solid or ice samples has recently been  
6 suggested by Spolaor *et al.* (Spolaor *et al.*, 2013). To illustrate this effect, Figure 4 shows the  
7 relation between the integrated infrared intensity on these bands for some pure samples  
8 irradiate at different temperatures, revealing the linear correlation existing between these  
9 values during the irradiation process (typical  $R^2$  value higher than 0.99). Note that this  
10 correlation is more difficult to examine in the case of  $\text{H}_2\text{O}$ /salt mixtures, since both i) the  
11 overlap of water and  $\text{IO}_3^-$  bands, ii) and the different changes that integrated absorption  
12 coefficients of  $\text{NH}_4^+$  and  $\text{IO}_3^-$  infrared bands could undergo in the presence of water, due to  
13 the intermolecular hydrogen bond formed in the hydration process. Nevertheless, and taking  
14 into account these considerations, the linear correlation (higher than 0.9) between both  
15 integral values can be observed in these cases, too, although it is not shown here.

16 Is important to highlight that not any evolution of the IR spectra of the samples was observed  
17 in dark conditions (this fact was checked many times along the experimental campaign).

18 Typical UV-Vis spectra of common ammonium salts (i.e.  $\text{NH}_4\text{Cl}$ ) do not display significant  
19 absorption bands in the near- UV and visible regions (see Fig. 2), and, to the best of our  
20 knowledge, no literature exists on the photolysis of this species. Based on this, the photolysis  
21 of ammonium ions is not expected to occur in this spectral range. Consequently, reduction of  
22 the IR ammonium bands should be caused by a fast reaction with “reacting” species produced  
23 by photolysis of frozen iodate during the irradiation process:  $\text{HOI}$ ,  $\text{IO}$  and  $\text{I}_2$  (Spolaor *et al.*,  
24 2013), or  $\text{OIO}$  (Klaning *et al.*, 1981), or other reacting species (e.g.: oxygen atoms or anions,  
25 see above). We observed that iodine reacts with ammonia in aqueous solution (McAlpine,  
26 1952), and consequently, we expected that any of these iodinated compounds obtained, which  
27 could be even more reactive than  $\text{I}_2$ , could react very fast with the present  $\text{NH}_4^+$ .

28 In addition to those at the 1430 and  $740\text{ cm}^{-1}$  bands, other changes are evident in the IR  
29 spectra, revealing that not only ammonium and iodate ions are consumed, but also new  
30 products are formed. These changes are more evident in the low temperature experiments,  
31 around 100 K, since volatile products formed during the photolysis can also be retained on the  
32 substrate. Figure 5 shows an example of a pure solid  $\text{NH}_4\text{IO}_3$  salt deposited at 100 K and



1 irradiated at that temperature. Dotted lines indicate bands that undergo clear changes during  
2 the photolysis.

3 Stretching of the  $\text{NH}_4^+$  bands around  $3000\text{ cm}^{-1}$  diminishes with irradiation, although an  
4 increase of water band intensities, more evident in the peak around  $3360\text{ cm}^{-1}$ , also occurs,  
5 probably due to the residual water background always present in the chamber (note that this  
6 effect only occurs at temperatures below 150 K). Two new peaks emerge during photolysis,  
7 around  $2227$  and  $1300\text{ cm}^{-1}$ . The first one is only visible at 100 K but the low frequency peak  
8 can also be observed at higher temperatures. The bands around  $2227\text{ cm}^{-1}$  could belong to  
9 infrared absorptions of C-O stretching modes. Slight carbon contamination mainly by  $\text{CO}_2$   
10 molecules are usually found in this type of experiments (Mate et al., 2014). Another  
11 possibility could be the formation of  $\text{N}_2\text{O}$  molecules which bear infrared signal around  $2200$   
12  $\text{cm}^{-1}$ . The band around  $1300\text{ cm}^{-1}$  can also be caused by N-O stretching vibration, which could  
13 be formed by reaction of  $\text{O}^*$  species with ammonium. Nevertheless, all these assignments  
14 should be considered as speculative.

15 According to the peaks observed as products in the IR spectra, the behaviour of reactant's IR  
16 peaks, and previous work on laser flash photolysis of iodate aqueous solution (Klaning et al.,  
17 1981) and photolysis of ice samples (Spolaor et al., 2013), we tentatively proposed some  
18 reactions that can occur in the photolysis of ammonium iodate ice, although further  
19 experiments to elucidate a complete mechanism are required:



22 OIO, IO, I and  $\text{I}_2$  or even HOI (by reaction of I or IO with OH/ $\text{HO}_2$ ) could be the active iodine  
23 products that are released to the atmosphere.  $\text{O}^-$  (in reaction R1) could be the activated specie  
24 that reacts with  $\text{NH}_4^+$ , or derivative, to consume it in a 1:1 ratio, although further studies are  
25 needed to clarify this point.

26 According to this mechanism, OIO is the initial iodine species formed. The IR band for this  
27 compound is about  $800\text{ cm}^{-1}$  (Maier and Bothur, 1997), and consequently, it cannot be  
28 monitored due to its overlap with the  $\text{IO}_3^-$  band. Nevertheless, as was mentioned above, more  
29 studies should be carried out to further understand the mechanism.

30 However, independently of the mechanism of the photolytic process, the photolytic rate  
31 constant,  $J$  value, for the iodate ion can be calculated according to equation E1:

$$1 \quad -\frac{d[IO_3^-]}{dt} = J[IO_3^-] \quad (E1)$$

2 The concentration of iodate ion can be monitored by integration of the infrared band intensity  
 3 at ca. 740 cm<sup>-1</sup>, that, as shown in Fig. 4, is equivalent to monitor the NH<sub>4</sub><sup>+</sup> band at 1430 cm<sup>-1</sup>:

$$4 \quad -\frac{d[IO_3^-]}{dt} = J[IO_3^-] \quad \ll == \gg \quad -\frac{d[NH_4^+]}{dt} = J[NH_4^+] \quad (E2)$$

5 Integrating E2 and considering that concentration is proportional to IR band intensity:

$$6 \quad \ln(I_t) = \ln(I_0) - Jt \quad (E3)$$

7 where  $I_t$  and  $I_0$  are the intensity of the band of NH<sub>4</sub><sup>+</sup> (or IO<sub>3</sub><sup>-</sup>) at time  $t$  and zero, respectively.

8 According to E3, a representation of the natural logarithm of the integrated band intensities of  
 9 NH<sub>4</sub><sup>+</sup> or IO<sub>3</sub><sup>-</sup> signals versus time of photolysis will give us the  $J$  value, as the slope of the line  
 10 of the best linear fit. This calculation has been done for all deposited samples at different  
 11 temperatures and water concentrations (see Figure 6 as an example for some of the samples).  
 12 Integration limits of the bands differ among the different samples, due to baseline of the  
 13 spectra are rather sensitive to the generation process and morphologies of the ices mixtures.  
 14 For this reason, the integration limits of the bands were adjusted for each sample studied in  
 15 order to minimize the errors during this process. The calculated mean value for all  
 16 experiments carried out (at an average light power of 0.66 W cm<sup>-2</sup>, see above) is  $J = (4 \pm 2) \times$   
 17  $10^{-5} \text{ s}^{-1}$ . Significant differences in the  $J$  values have not been observed among the samples  
 18 prepared at different conditions, i.e. *Vap* o *HQ* deposition of water, different water ice  
 19 structure (amorphous or cubic), different temperatures of generation and irradiation (from 100  
 20 to 298 K) or different amount of water in the mixtures, although in this last case, for more  
 21 diluted samples the resulting  $J$  values are usually higher in absolute terms (the average  $J$  value  
 22 considering only diluted samples is around 10 % higher). This effect could be due to a larger  
 23 surface/bulk ratio in diluted samples, although in any case, it is always within the  
 24 experimental uncertainties. The fact that not significant variations on the calculated  $J$  values  
 25 were obtaining in the experiments point to the photo-reduction process do not notably  
 26 depends on the morphology of the ices, or even the amorphous or crystalline structure, at least  
 27 in the range of samples studied.

28 If the photolysis rate and the radiative flux are known, the integrated cross section of the  
 29 iodate ion can be estimated according to E4:

$$J = \int_{\lambda_1}^{\lambda_2} F(\lambda)\sigma(\lambda)\phi(\lambda)d\lambda \quad (\text{E4})$$

where  $F(\lambda)$  is the radiative flux,  $\sigma(\lambda)$  is the absorption cross section and  $\phi(\lambda)$  is the quantum yield of the photolysis reaction. The radiative flux employed in the experiment has been calculated previously (see experimental section). If we assume a constant quantum yield of unity in the interval, the integrated absorption cross section from 300 to 900 nm yields a value of  $(1.1 \pm 0.6) \times 10^{-20} \text{ cm}^2 \text{ nm}$ . For comparison purposes, the integrated cross section of  $\text{O}_3$  in the spectral interval 410–690 nm (Chappuis band) is around  $6.6 \times 10^{-20} \text{ cm}^2 \text{ nm}$  (Bogumil et al., 2001).

The assumption of a constant quantum yield of unity in the interval should be regarded with caution. It is known that this value depends not only on the wavelength value but the dilution and conditions of the samples, too (as for example on their aggregation phase) (Rahn et al., 2003). However, there is no information about this value for any frozen iodate frozen salt, and in consequence the integrated cross section determined in this study assumes that the quantum yield of the photolysis process. This assumption has to be taken into account in order to use this integrated cross section value for any purpose.

In order to estimate the near visible absorption of iodate salts, UV-Vis spectra were recorded for water solution of  $\text{NH}_4\text{IO}_3$ ,  $\text{NH}_4\text{Cl}$  and  $\text{KIO}_3$  salts (see Fig. 2). In all cases, nearly null absorptions were recorded above 300 nm. These results are in agreement with that of Saunders *et al.*, (Saunders et al., 2012) and Awtrey and Connick, (Awtrey and Connick, 1951), who also found nearly null absorption above 300 nm for  $\text{NaIO}_3$  salt solutions. According to these results, the photo-reactivity of the iodate salts should be related to the low-temperature effect, and the fact that iodate solutions or salts are frozen, in agreement with the results from Spolaor *et al.* (Spolaor et al., 2013). It is well known that different photochemical reactions are greatly accelerated in frozen solution due, for example, by the concentration of solutes in porous or channel formed in the water ice network (see e.g. Grannas *et al.* (Grannas et al., 2007) and references therein).

In order to model the influence of the photolytic process of iodate in the polar environment, it could be more convenient to use an estimation of the variation of the absorption cross section, instead of the integrated cross section measured, due to the large variation of the spectral actinic flux in this interval. With this aim, we provide an estimation of the variation of the absorption cross section, using as a reference the spectral shape of the  $\text{NH}_4\text{IO}_3$  solutions

1 showed in Fig. 2. According to this, it seems reasonable to approximate the spectral shape to a  
2 decay tail of a Gaussian function (although no significant differences would be obtained if a  
3 Lorentzian function would be used) peaking in 205 nm (according to the spectrum of  $9.6 \times 10^{-4}$   
4 M  $\text{NH}_4\text{IO}_3$  shown in Figure 2), which is presented in Fig. 7. The total area of the Gaussian  
5 function simulation (from 300 to 900 nm) has been fixed to the previous calculated value for  
6 the integrated absorption cross section, and the width of the Gaussian function has arbitrarily  
7 selected to force that approx. 95 % of the value of the integrated cross section would be in the  
8 range from 300 to 500 nm. In this calculation, a  $\sigma$  of  $1.35 \times 10^{-22} \text{ cm}^2$  is obtained at 350 nm, a  
9 value, for example, relatively close to that recorded for  $\text{O}_3$  at this frequency, approx.  $4 \times 10^{-22}$   
10  $\text{cm}^2$  (Burrows et al., 1999), but quite far lower than the one for  $\text{NO}_3$  at 662 nm that is  $1.90 \times$   
11  $10^{-17} \text{ cm}^2$  at 298 K (Ravishankara and Mauldin, 1986).

12 However, due to the above mentioned limitations in our experimental set-up the integrated  
13 absorption cross-section of iodate should be regarded as a lower limit. The reason is mainly  
14 the limitations associated with distributing the samples homogeneously during deposition,  
15 which could generate areas free of samples on the substrate. For these cases, the irradiance  
16 received by the samples could be lower than calculated (which assume a homogeneous  
17 distribution of the sample), leading finally to a higher calculated absorption cross section  
18 value than the one obtained in this work. Based on the dispersion of our results, we have  
19 estimated that this effect could account for an increase on this value by up to a factor of two.  
20 In addition, diluted samples showed an increase of the  $J$  values of around 10 %, which,  
21 although in within experimental limitations, also would cause a higher absorption cross  
22 section value. In conclusion, both effects could account for a cross section value up to an  
23 order of magnitude higher than that reported here, so we emphasize that it should be  
24 considered as a lower limit. Nevertheless, further experiments should be done to confirm the  
25 integrated absorption cross section value.

26

### 27 **3.2 Model simulations**

28 In spite of the experimental limitations mentioned above, we have incorporated the  
29 experimentally-derived absorption cross section value into an atmospheric model in order to  
30 assess the implications that this process could have in polar atmospheric chemistry.

1 Although high levels of reactive iodine have been measured in coastal Antarctica, the  
2 emission mechanism over ice still remains unclear. We use an atmospheric model (for details  
3 see Saiz-Lopez et al.(Saiz-Lopez et al., 2008)) of the Antarctic boundary layer to assess the  
4 potential of iodate photolysis to release reactive iodine to the polar atmosphere. The model is  
5 initialized with typical concentrations of atmospheric constituents in coastal Antarctica (Jones  
6 et al., 2008) for October. We constrain the ice surface in the model with an average iodate  
7 concentration at the ice surface of 19 nM, as recently measured over the Weddell Sea  
8 (Atkinson et al., 2012). The model incorporates a 2-stream radiation code to compute the  
9 actinic flux at the surface for springtime Antarctic irradiation conditions (Saiz-Lopez et al.,  
10 2008), and the mean iodate integrated absorption cross section estimated in this work, which  
11 again recall that it is a lower limit. We assume that there is an iodine atom unity conversion of  
12 iodate into reactive gas phase following iodate photolysis. The model results indicate that the  
13 photoreduction of iodate in ice, and subsequent equilibration of the reactive iodine species,  
14 yields atmospheric IO levels around 1-1.5 pptv. These levels of IO are lower than the highest  
15 values measured in the biologically-active Weddell Sea region. However, lower IO  
16 concentrations have also been reported in other coastal regions away from the Weddell Sea  
17 (Schönhardt et al., 2008). We would like to highlight that the IO concentration given by the  
18 model is proportional to the cross section values used for iodate, so much larger IO levels  
19 could be obtained. The photolysis of iodate could provide a source of iodine that accounts for  
20 some of the comparatively low levels observed, and, to a lesser extent, also contribute to the  
21 iodine emissions over the Weddell Sea zone. Note that the model does not consider the  
22 potential loss at the ice surface of the iodine photofragments resulting from the iodate  
23 photolysis. The model results suggest, within the uncertainties highlighted above, that the  
24 photolysis of iodate on the surface of ice can potentially constitute an abiotic pathway for the  
25 release of active iodine to the polar atmosphere. Further laboratory and field work is needed  
26 to better assess the environmental implications of iodate photolysis in the ice.

27

#### 28 **4 Conclusions**

29 We have explored the photolysis of ammonium iodate salt in frozen solutions. The samples  
30 were generated by different deposition methods, and at different temperatures and water  
31 concentrations, in order to obtain samples of different morphologies. The samples were  
32 processed by simulated Solar light with an average light power of  $0.66 \text{ W cm}^{-2}$ , in the

1 wavelength range of 300 to 900 nm. In all cases, the evolution of the IR spectra confirms the  
2 photolysis of iodate salt for all samples in a similar way. The photolysis rates obtained are  
3 similar for all the samples generated, within our experimental uncertainties, indicating that in  
4 the photolytic process there is a limited influence of the morphology and structure of the  
5 water ice matrix. The bands of  $\text{NH}_4^+$  and  $\text{IO}_3^-$  decrease during irradiation and new small bands  
6 appear, too. Some relevant reactions of the photolysis process are presented, in which OIO is  
7 formed as a first step of the photolysis of iodate. Both OIO and other reactive iodine species,  
8 which could be formed in subsequent reactions (IO,  $\text{I}_2$ , HOI, etc.), could be released to the gas  
9 phase. As result of these experiments, the integrated absorption cross section of iodate in an  
10 ammonium frozen salt has been estimated for the first time at wavelengths relevant for  
11 tropospheric studies ( $\sigma = (1.1 \pm 0.6) \times 10^{-20} \text{ cm}^2 \text{ nm}$  from 300 to 900 nm). However, due to  
12 the experimental limitations, this value has to be considered mainly as a lower limit, and  
13 further experiments are needed to confirm it. A simulated absorption cross section in this  
14 interval region has also been proposed, which has been included in an atmospheric model of  
15 the Antarctic boundary layer to assess its potential environmental relevance. The model  
16 predicts that the photolysis of iodate in ice could yield atmospheric IO levels around 1-1.5  
17 pptv, which could be higher if we consider a larger absorption cross sections value for the  
18 photolysis of iodate. According to this, we suggest that the photolysis of iodate on the surface  
19 of ice can potentially constitute a pathway for the release of active iodine to the polar  
20 atmosphere.

21

## 22 **Acknowledgements**

23 O. G. acknowledges financial support from Ministerio de Ciencia e Innovación, “Ramón y  
24 Cajal” program and financial support from Ministerio de Economía y Competitividad, project  
25 “CGL2013-48415-C2-1-R”. M.T.B-R and M.S. acknowledge financial support from  
26 Ministerio de Economía y Competitividad, project “CGL2013-48415-C2-2”. O. G., M.T.B-R  
27 and M.S. acknowledge financial support from the Spanish crowdfunding platform  
28 PRECIPITA from FECYT foundation.

29

30

## 1 References

- 2 Abad, L., Bermejo, D., Herrero, V. J., Santos, J., and Tanarro, I.: Performance of a solenoid-  
3 driven pulsed molecular-beam source, *Review of Scientific Instruments*, 66, 3826-3832,  
4 doi:<http://dx.doi.org/10.1063/1.1145444>, 1995.
- 5 Allan, J. D., Williams, P. I., Najera, J., Whitehead, J. D., Flynn, M. J., Taylor, J. W., Liu, D.,  
6 Darbyshire, E., Carpenter, L. J., Chance, R., Andrews, S. J., Hackenberg, S. C., and  
7 McFiggans, G.: Iodine observed in new particle formation events in the Arctic atmosphere  
8 during ACCACIA, *Atmos. Chem. Phys.*, 15, 5599-5609, 10.5194/acp-15-5599-2015, 2015.
- 9 Assmy, P., Ehn, J. K., Fernández-Méndez, M., Hop, H., Katlein, C., Sundfjord, A., Bluhm,  
10 K., Daase, M., Engel, A., Fransson, A., Granskog, M. A., Hudson, S. R., Kristiansen, S.,  
11 Nicolaus, M., Peeken, I., Renner, A. H. H., Spreen, G., Tatarek, A., and Wiktor, J.: Floating  
12 Ice-Algal Aggregates below Melting Arctic Sea Ice, *PLoS ONE*, 8, e76599,  
13 10.1371/journal.pone.0076599, 2013.
- 14 Atkinson, H. M., Huang, R. J., Chance, R., Roscoe, H. K., Hughes, C., Davison, B.,  
15 Schönhardt, A., Mahajan, A. S., Saiz-Lopez, A., Hoffmann, T., and Liss, P. S.: Iodine  
16 emissions from the sea ice of the Weddell Sea, *Atmos. Chem. Phys.*, 12, 11229-11244,  
17 10.5194/acp-12-11229-2012, 2012.
- 18 Awtrey, A. D., and Connick, R. E.: The Absorption Spectra of  $I_2$ ,  $I_3^-$ ,  $I$ ,  $IO_3^-$ ,  $S_4O_6^{=}$  and  $S_2O_3^{=}$ .  
19 Heat of the Reaction  $I_3^- = I_2 + I$ , *Journal of the American Chemical Society*, 73, 1842-1843,  
20 10.1021/ja01148a504, 1951.
- 21 Baker, A. R., Thompson, D., Campos, M. L. A. M., Parry, S. J., and Jickells, T. D.: Iodine  
22 concentration and availability in atmospheric aerosol, *Atmospheric Environment*, 34, 4331-  
23 4336, [http://dx.doi.org/10.1016/S1352-2310\(00\)00208-9](http://dx.doi.org/10.1016/S1352-2310(00)00208-9), 2000.
- 24 Baker, A. R.: Inorganic iodine speciation in tropical Atlantic aerosol, *Geophysical Research*  
25 *Letters*, 31, n/a-n/a, 10.1029/2004gl020144, 2004.
- 26 Bogumil, K., Orphal, J., Burrows, J. P., and Flaud, J. M.: Vibrational progressions in the  
27 visible and near-ultraviolet absorption spectrum of ozone, *Chemical Physics Letters*, 349,  
28 241-248, [http://dx.doi.org/10.1016/S0009-2614\(01\)01191-5](http://dx.doi.org/10.1016/S0009-2614(01)01191-5), 2001.
- 29 Burrows, J. P., Richter, A., Dehn, A., Deters, B., Himmelmann, S., Voigt, S., and Orphal, J.:  
30 Atmospheric remote-sensing reference data from GOME---2. Temperature-dependent  
31 absorption cross sections of O<sub>3</sub> in the 231-794 nm range, *Journal of Quantitative*  
32 *Spectroscopy and Radiative Transfer*, 61, 509-517, [http://dx.doi.org/10.1016/S0022-](http://dx.doi.org/10.1016/S0022-4073(98)00037-5)  
33 [4073\(98\)00037-5](http://dx.doi.org/10.1016/S0022-4073(98)00037-5), 1999.
- 34 Calvert, J. G., and Lindberg, S. E.: The potential influence of iodine-containing compounds  
35 on the chemistry of the troposphere in the polar spring. II. Mercury depletion, *Atmospheric*  
36 *Environment*, 38, 5105-5116, <http://dx.doi.org/10.1016/j.atmosenv.2004.05.050>, 2004.
- 37 Frieß, U., Wagner, T., Pundt, I., Pfeilsticker, K., and Platt, U.: Spectroscopic measurements of  
38 tropospheric iodine oxide at Neumayer Station, Antarctica, *Geophysical Research Letters*, 28,  
39 1941-1944, 10.1029/2000gl012784, 2001.
- 40 Gálvez, O., Maté, B., Herrero, V. J., and Escribano, R.: Ammonium and Formate Ions in  
41 Interstellar Ice Analogs, *The Astrophysical Journal*, 724, 539, 2010.
- 42 Gálvez, Ó., Maté, B., Martín-Llorente, B., Herrero, V. J., and Escribano, R.: Phases of Solid  
43 Methanol, *The Journal of Physical Chemistry A*, 113, 3321-3329, 10.1021/jp810239r, 2009.

1 Gilfedder, B. S., Lai, S. C., Petri, M., Biester, H., and Hoffmann, T.: Iodine speciation in rain,  
2 snow and aerosols, *Atmos. Chem. Phys.*, 8, 6069-6084, 10.5194/acp-8-6069-2008, 2008.

3 Grannas, A. M., Jones, A. E., Dibb, J., Ammann, M., Anastasio, C., Beine, H. J., Bergin, M.,  
4 Bottenheim, J., Boxe, C. S., Carver, G., Chen, G., Crawford, J. H., Dominé, F., Frey, M. M.,  
5 Guzmán, M. I., Heard, D. E., Helmig, D., Hoffmann, M. R., Honrath, R. E., Huey, L. G.,  
6 Hutterli, M., Jacobi, H. W., Klán, P., Lefer, B., McConnell, J., Plane, J., Sander, R., Savarino,  
7 J., Shepson, P. B., Simpson, W. R., Sodeau, J. R., von Glasow, R., Weller, R., Wolff, E. W.,  
8 and Zhu, T.: An overview of snow photochemistry: evidence, mechanisms and impacts,  
9 *Atmos. Chem. Phys.*, 7, 4329-4373, 10.5194/acp-7-4329-2007, 2007.

10 Jones, A. E., Wolff, E. W., Salmon, R. A., Bauguitte, S. J. B., Roscoe, H. K., Anderson, P. S.,  
11 Ames, D., Clemitshaw, K. C., Fleming, Z. L., Bloss, W. J., Heard, D. E., Lee, J. D., Read, K.  
12 A., Hamer, P., Shallcross, D. E., Jackson, A. V., Walker, S. L., Lewis, A. C., Mills, G. P.,  
13 Plane, J. M. C., Saiz-Lopez, A., Sturges, W. T., and Worton, D. R.: Chemistry of the  
14 Antarctic Boundary Layer and the Interface with Snow: an overview of the CHABLIS  
15 campaign, *Atmos. Chem. Phys.*, 8, 3789-3803, 10.5194/acp-8-3789-2008, 2008.

16 Kim, K., Yabushita, A., Okumura, M., Saiz-Lopez, A., Cuevas, C. A., Blaszcak-Boxe, C. S.,  
17 Min, D. W., Yoon, H.-I., and Choi, W.: Production of molecular iodine and triiodide in the  
18 frozen solution of iodide: implication for polar atmosphere, *Environmental Science &*  
19 *Technology*, 10.1021/acs.est.5b05148, 2016.

20 Klaning, U. K., Sehested, K., and Wolff, T.: Laser flash photolysis and pulse radiolysis of  
21 iodate and periodate in aqueous solution. Properties of iodine(VI), *Journal of the Chemical*  
22 *Society, Faraday Transactions 1: Physical Chemistry in Condensed Phases*, 77, 1707-1718,  
23 10.1039/f19817701707, 1981.

24 Laniewski, K., Borén, H., and Grimvall, A.: Fractionation of halogenated organic matter  
25 present in rain and snow, *Chemosphere*, 38, 393-409, [http://dx.doi.org/10.1016/S0045-](http://dx.doi.org/10.1016/S0045-6535(98)00181-7)  
26 [6535\(98\)00181-7](http://dx.doi.org/10.1016/S0045-6535(98)00181-7), 1999.

27 Maier, G., and Bothur, A.: Matrix-Isolation of Iodine Superoxide and Iodine Dioxide,  
28 *Chemische Berichte*, 130, 179-181, 10.1002/cber.19971300207, 1997.

29 Mastrapa, R. M., Sandford, R. M., Roush, T. L., Cruikshank, D. P., and Dalle Ore, C. M.:  
30 Optical Constants of Amorphous and Crystalline H<sub>2</sub>O-ice: 2.5-22  $\mu\text{m}$  (4000-455  $\text{cm}^{-1}$ )  
31 Optical Constants of H<sub>2</sub>O-ice, *The Astrophysical Journal*, 701, 1347, 2009.

32 Mate, B., Rodriguez-Lazcano, Y., and Herrero, V. J.: Morphology and crystallization kinetics  
33 of compact (HGW) and porous (ASW) amorphous water ice, *Physical Chemistry Chemical*  
34 *Physics*, 14, 10595-10602, 10.1039/c2cp41597f, 2012.

35 Mate, B., Tanarro, I., Moreno, M. A., Jimenez-Redondo, M., Escribano, R., and Herrero, V.  
36 J.: Stability of carbonaceous dust analogues and glycine under UV irradiation and electron  
37 bombardment, *Faraday Discussions*, 168, 267-285, 10.1039/c3fd00132f, 2014.

38 Maté, B., Gálvez, O., Herrero, V. J., Fernández-Torre, D., Moreno, M. A., and Escribano, R.:  
39 Water-Ammonium ICES and the Elusive 6.85  $\mu\text{m}$  Band, *The Astrophysical Journal Letters*,  
40 703, L178, 2009.

41 Mayer, E.: New method for vitrifying water and other liquids by rapid cooling of their  
42 aerosols, *Journal of Applied Physics*, 58, 663-667, doi:<http://dx.doi.org/10.1063/1.336179>,  
43 1985.



1 McAlpine, R. K.: The Reaction of Dilute Iodine and Ammonia Solutions, *Journal of the*  
2 *American Chemical Society*, 74, 725-727, 10.1021/ja01123a041, 1952.

3 Ocampo, J., and Klinger, J.: Adsorption of N<sub>2</sub> and CO<sub>2</sub> on ice, *Journal of Colloid and*  
4 *Interface Science*, 86, 377-383, [http://dx.doi.org/10.1016/0021-9797\(82\)90083-2](http://dx.doi.org/10.1016/0021-9797(82)90083-2), 1982.

5 Pechtl, S., Lovejoy, E. R., Burkholder, J. B., and von Glasow, R.: Modeling the possible role  
6 of iodine oxides in atmospheric new particle formation, *Atmos. Chem. Phys.*, 6, 505-523,  
7 10.5194/acp-6-505-2006, 2006.

8 Rahn, R. O., Stefan, M. I., Bolton, J. R., Goren, E., Shaw, P.-S., and Lykke, K. R.: Quantum  
9 Yield of the Iodide–Iodate Chemical Actinometer: Dependence on Wavelength and  
10 Concentration¶, *Photochemistry and Photobiology*, 78, 146-152, 10.1562/0031-  
11 8655(2003)0780146qyotic2.0.co2, 2003.

12 Ravishankara, A. R., and Mauldin, R. L.: Temperature dependence of the NO<sub>3</sub> cross section  
13 in the 662-nm region, *Journal of Geophysical Research: Atmospheres*, 91, 8709-8712,  
14 10.1029/JD091iD08p08709, 1986.

15 Read, K. A., Mahajan, A. S., Carpenter, L. J., Evans, M. J., Faria, B. V. E., Heard, D. E.,  
16 Hopkins, J. R., Lee, J. D., Moller, S. J., Lewis, A. C., Mendes, L., McQuaid, J. B., Oetjen, H.,  
17 Saiz-Lopez, A., Pilling, M. J., and Plane, J. M. C.: Extensive halogen-mediated ozone  
18 destruction over the tropical Atlantic Ocean, *Nature*, 453, 1232-1235,  
19 [http://www.nature.com/nature/journal/v453/n7199/supinfo/nature07035\\_S1.html](http://www.nature.com/nature/journal/v453/n7199/supinfo/nature07035_S1.html), 2008.

20 Roscoe, H. K., Jones, A. E., Brough, N., Weller, R., Saiz-Lopez, A., Mahajan, A. S.,  
21 Schoenhardt, A., Burrows, J. P., and Fleming, Z. L.: Particles and iodine compounds in  
22 coastal Antarctica, *Journal of Geophysical Research: Atmospheres*, 120, 7144-7156,  
23 10.1002/2015jd023301, 2015.

24 Saiz-Lopez, A., Chance, K., Liu, X., Kurosu, T. P., and Sander, S. P.: First observations of  
25 iodine oxide from space, *Geophysical Research Letters*, 34, n/a-n/a, 10.1029/2007gl030111,  
26 2007a.

27 Saiz-Lopez, A., Mahajan, A. S., Salmon, R. A., Bauguitte, S. J.-B., Jones, A. E., Roscoe, H.  
28 K., and Plane, J. M. C.: Boundary Layer Halogens in Coastal Antarctica, *Science*, 317, 348-  
29 351, 10.1126/science.1141408, 2007b.

30 Saiz-Lopez, A., Plane, J. M. C., Mahajan, A. S., Anderson, P. S., Bauguitte, S. J. B., Jones, A.  
31 E., Roscoe, H. K., Salmon, R. A., Bloss, W. J., Lee, J. D., and Heard, D. E.: On the vertical  
32 distribution of boundary layer halogens over coastal Antarctica: implications for O<sub>3</sub>, HO<sub>x</sub>,  
33 NO<sub>x</sub> and the Hg lifetime, *Atmos. Chem. Phys.*, 8, 887-900, 10.5194/acp-8-887-2008, 2008.

34 Saiz-Lopez, A., Plane, J. M. C., Baker, A. R., Carpenter, L. J., von Glasow, R., Gómez  
35 Martín, J. C., McFiggans, G., and Saunders, R. W.: Atmospheric Chemistry of Iodine,  
36 *Chemical Reviews*, 112, 1773-1804, 10.1021/cr200029u, 2012.

37 Saiz-Lopez, A., Blaszczyk-Boxe, C. S., and Carpenter, L. J.: A mechanism for biologically-  
38 induced iodine emissions from sea-ice, *Atmos. Chem. Phys.*, 15, 9731-9746, 10.5194/acp-15-  
39 9731-2015, 2015.

40 Saunders, R. W., Kumar, R., MacDonald, S. M., and Plane, J. M. C.: Insights into the  
41 Photochemical Transformation of Iodine in Aqueous Systems: Humic Acid Photosensitized  
42 Reduction of Iodate, *Environmental Science & Technology*, 46, 11854-11861,  
43 10.1021/es3030935, 2012.

- 1 Schönhardt, A., Richter, A., Wittrock, F., Kirk, H., Oetjen, H., Roscoe, H. K., and Burrows, J.  
2 P.: Observations of iodine monoxide columns from satellite, *Atmos. Chem. Phys.*, 8, 637-653,  
3 10.5194/acp-8-637-2008, 2008.
- 4 Schutte, W. A., and Khanna, R. K.: Origin of the 6.85 micron band near young stellar objects:  
5 The ammonium ion (NH<sub>4</sub><sup>+</sup>) revisited, *A&A*, 398, 1049-1062, 2003.
- 6 Spolaor, A., Vallelonga, P., Plane, J. M. C., Kehrwald, N., Gabrieli, J., Varin, C., Turetta, C.,  
7 Cozzi, G., Kumar, R., Boutron, C., and Barbante, C.: Halogen species record Antarctic sea ice  
8 extent over glacial–interglacial periods, *Atmos. Chem. Phys.*, 13, 6623-6635, 10.5194/acp-13-  
9 6623-2013, 2013.
- 10  
11  
12  
13

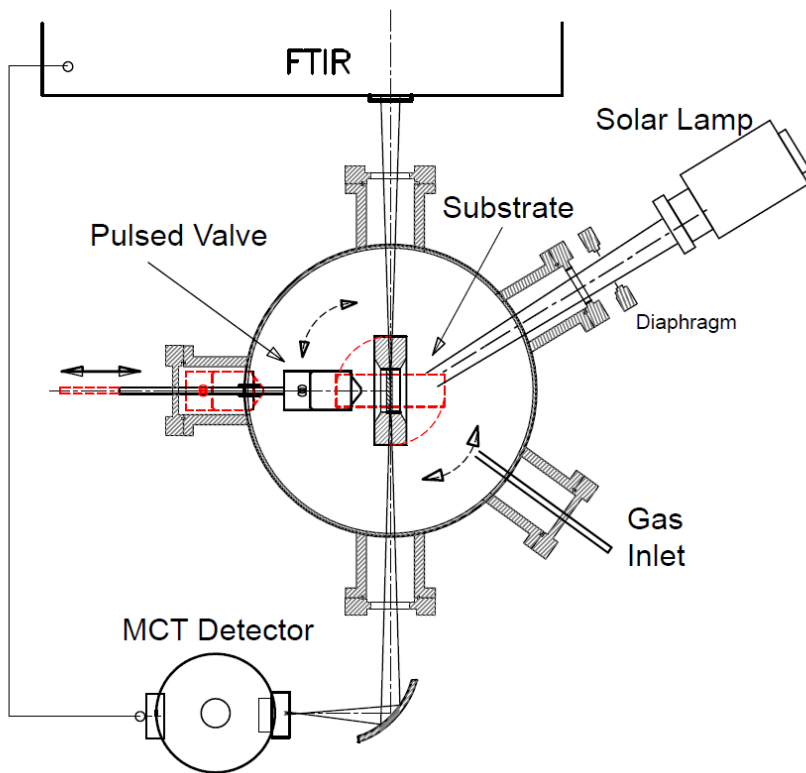
1 **Table 1.** Positions (in  $\text{cm}^{-1}$ ) and assignment of the mid-IR spectra bands of the  $\text{NH}_4\text{IO}_3$  salt  
 2 shown in Fig. 2.

Experiment	$\nu_1, \nu_3 (\text{IO}_3^-)$	$\nu_4 (\text{NH}_4^+)$	$2\nu_1, \nu_3 (\text{IO}_3^-)?$	$2\nu_4, \nu_2 + \nu_4, \nu_3 (\text{NH}_4^+)$
$\text{NH}_4\text{IO}_3$ 200 K	742, 792 <sup>sh</sup>	1428, 1451 <sup>sh</sup>	1683	2839, 3020, 3165
$\text{NH}_4\text{IO}_3$ 100 K	738, 772 <sup>sh</sup> , 792 <sup>sh</sup>	1432, 1456 <sup>sh</sup>	1683	2839, 3020, 3154
3.6 $\text{H}_2\text{O}/\text{NH}_4\text{IO}_3$ 100 K HQ	745, 769 <sup>sh</sup> , 794 <sup>sh</sup>	1432, 1456 <sup>sh</sup>	1683	2839, 3020, 3154 <sup>sh</sup>
2.1 $\text{H}_2\text{O}/\text{NH}_4\text{IO}_3$ 100 K Vap	749, 792 <sup>sh</sup>	1432, 1456 <sup>sh</sup>	1683	2839, 3020, 3154 <sup>sh</sup>

3

4

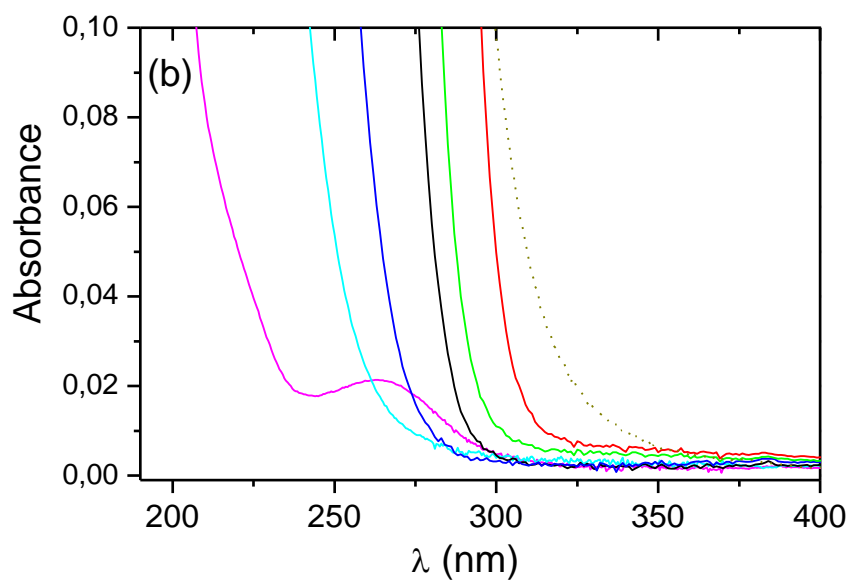
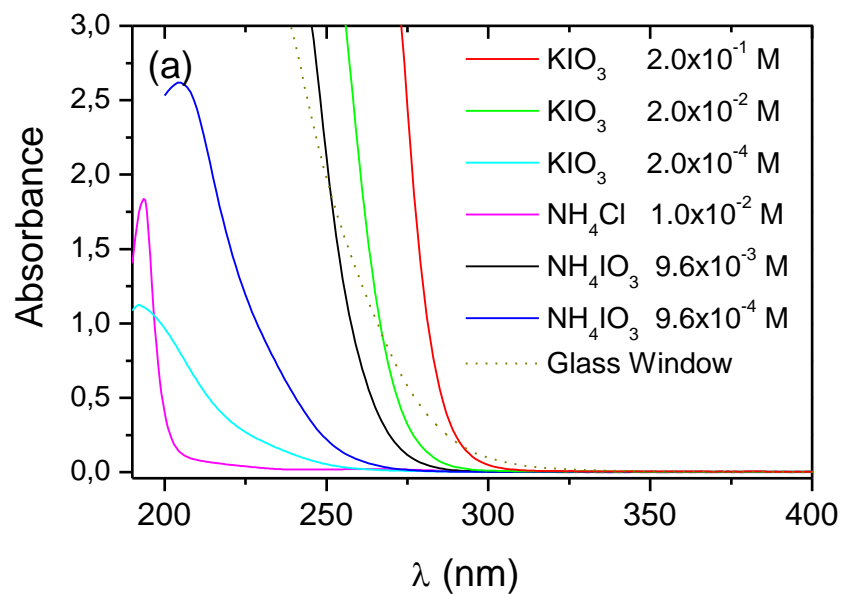
5



1

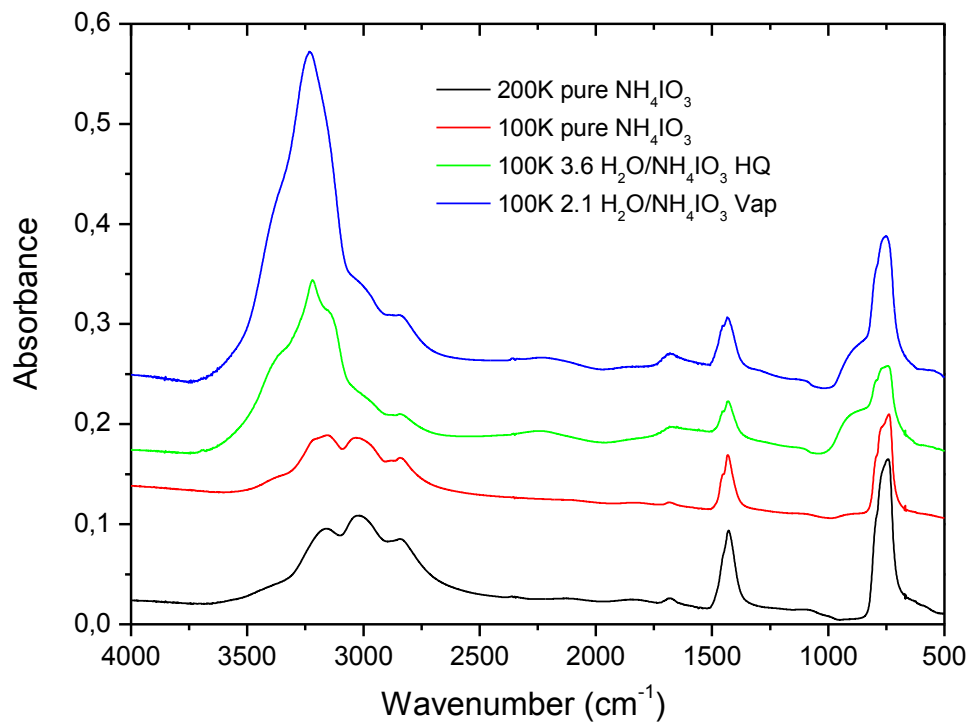
2 **Figure 1.** Schematic view of the experimental setup.

3



1  
2  
3  
4  
5  
6

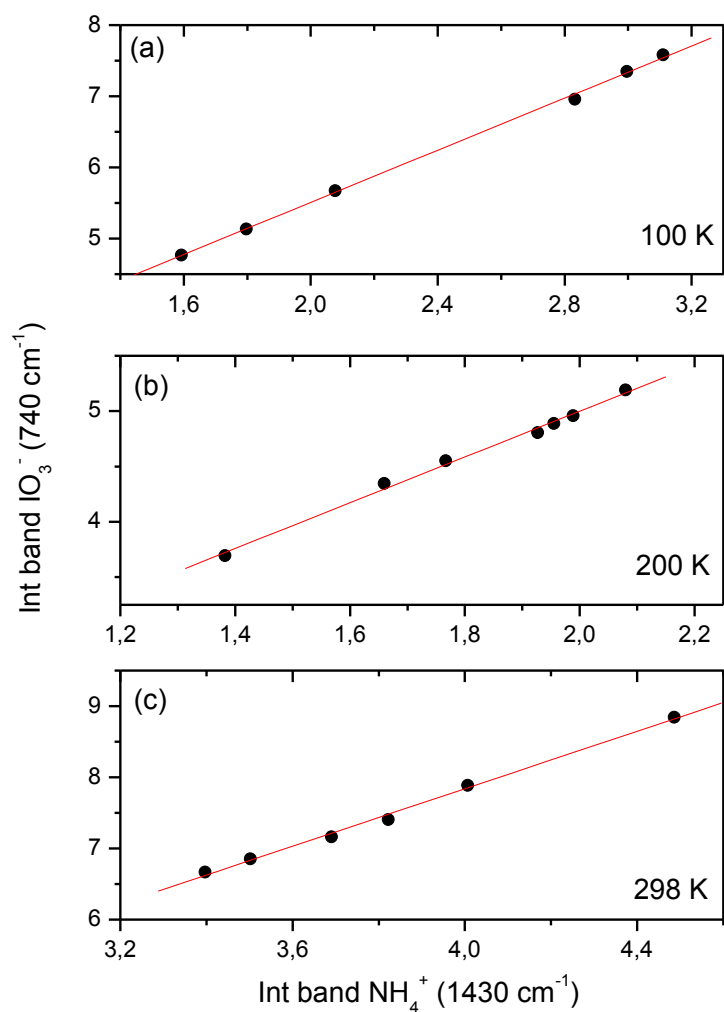
**Figure 2.** (a) UV-Vis absorption spectra from 190 to 400 nm for  $\text{KIO}_3$ ,  $\text{NH}_4\text{Cl}$  and  $\text{NH}_4\text{IO}_3$  aqueous solutions. (b) Zoom-in of the low absorbance values.



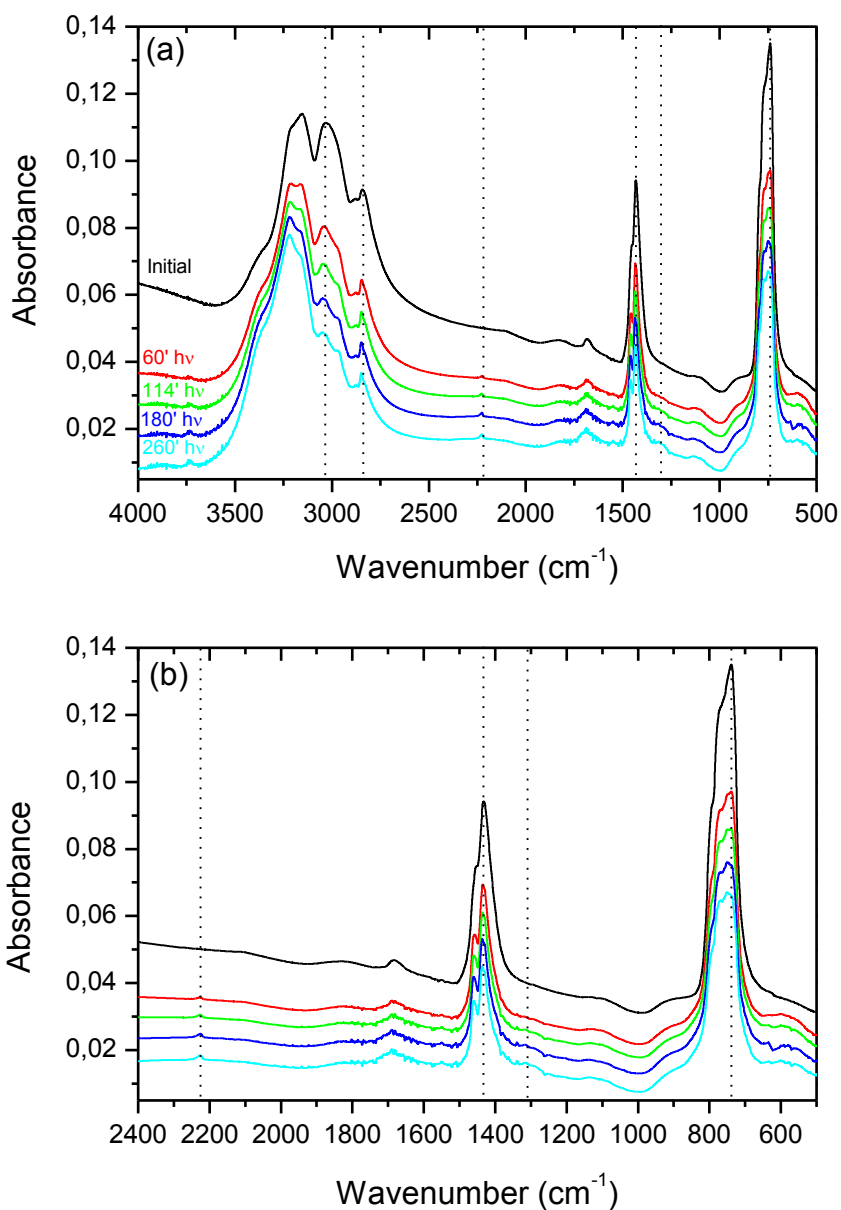
1  
2

3 **Figure 3.** Mid-IR transmission spectra of pure NH<sub>4</sub>IO<sub>3</sub> and H<sub>2</sub>O/NH<sub>4</sub>IO<sub>3</sub> ice mixtures  
4 generated at different temperatures.

5



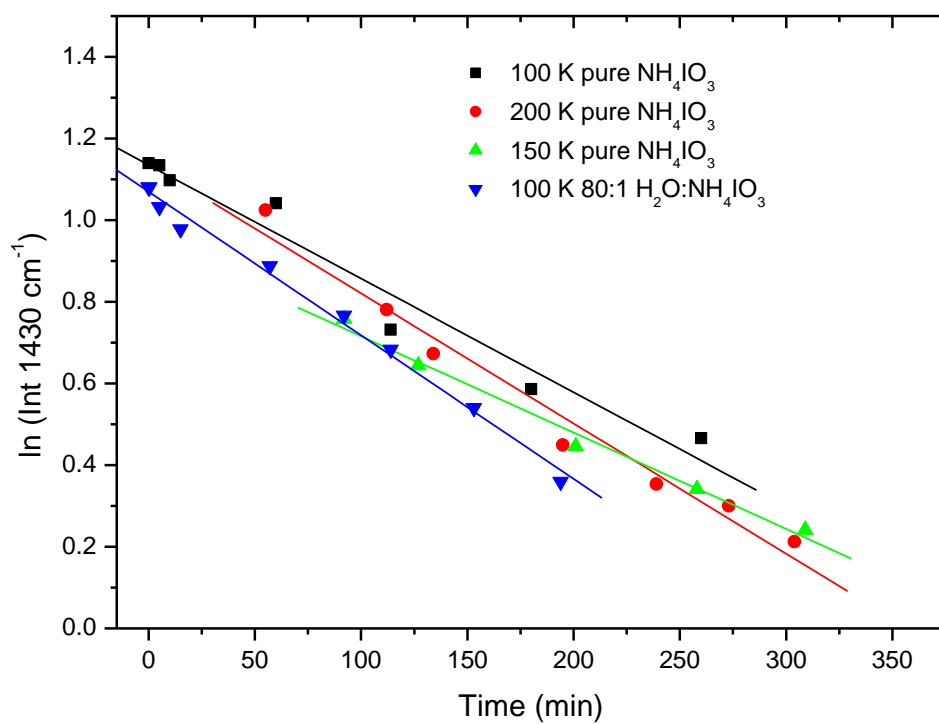
1  
 2 **Figure 4.** Integrated intensities (in arbitrary units) of the  $v_4$  band of  $\text{NH}_4^+$  and the  $v_3$  of  $\text{IO}_3^-$  of  
 3 pure ammonium iodate samples generated and irradiated at (a) 100 K (b) 200 K and (c) 298  
 4 K. Fit linear regression lines are shown in red.  
 5



1  
 2 **Figure 5.** Evolution of the mid-IR transmission spectra of a pure  $\text{NH}_4\text{IO}_3$  deposited at 100 K  
 3 during photolysis at that temperature: Zero time, 60, 114, 180 and 260 min of photolysis in  
 4 black, red, green, dark and light blue, respectively. The upper panel shows the whole IR  
 5 spectra between 4000 and 500  $\text{cm}^{-1}$ , the bottom panel is a zoom in the range 2400-600  $\text{cm}^{-1}$ .  
 6 Dotted lines indicate bands that undergo clear changes during the photolysis.

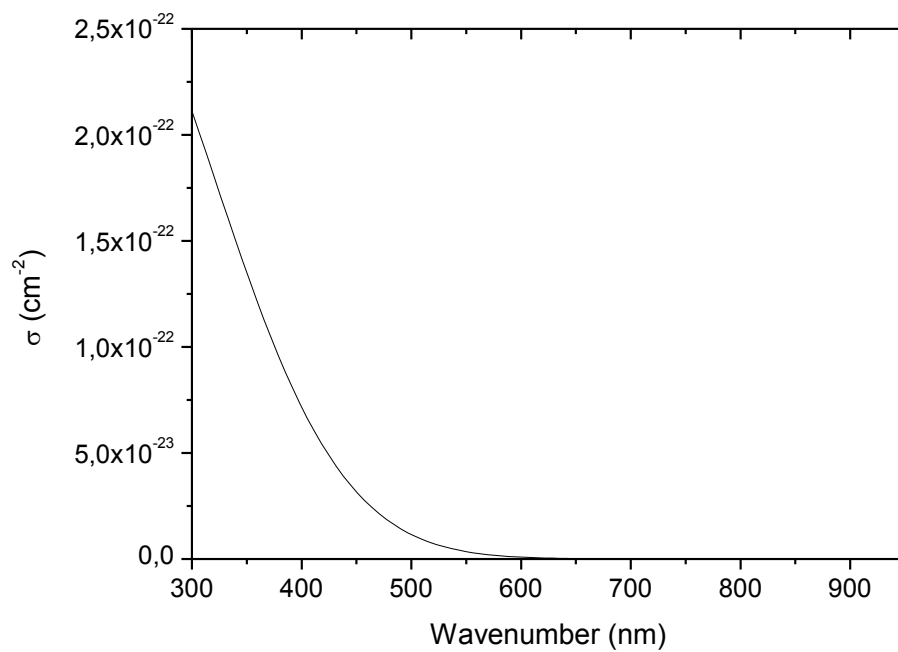
7





1  
 2 **Figure 6.** Representation of the natural logarithm of the integrated band intensity of  $\text{NH}_4^+$  at  
 3  $1430\text{ cm}^{-1}$  band versus photolysis time for some selected samples generated and irradiated at  
 4 different temperatures.

5  
 6



1

2 **Figure 7.** Simulated absorption cross section of iodate ion in a frozen ammonium iodate salt.

3